Engineering Structures 69 (2014) 102–115

Contents lists available at ScienceDirect

Engineering Structures

journal homepage: www.elsevier.com/locate/engstruct

Experimental analysis of seismic resistance of timber-framed structures with stones and earth infill

F. Vieux-Champagne [a,b,*], Y. Sieffert [a,b], S. Grange [a,b], A. Polastri [c], A. Ceccotti [c], L. Daudeville [a,b]

[a] Univ. Grenoble Alpes, 3SR, F-38000 Grenoble, France
[b] CNRS, 3SR, F-38000 Grenoble, France
[c] CNR IVALSA, Via Biasi 75, San Michele all'Adige, Italy

ARTICLE INFO

Article history:
Received 22 July 2013
Revised 7 February 2014
Accepted 24 February 2014

Keywords:
Timber-framed structures
Timbered masonry
Earth
Stones
Infill
Seismic resistant
Hysteretic behavior
Multi-scale approach
Equivalent viscous damping

ABSTRACT

The seismic performance of timber-framed structures filled with natural stones and earth mortar is analyzed by introducing three scales of experiments during which both cyclic and monotonic loadings are considered. At the connection scale, tests are performed in both normal and tangential directions to obtain the hysteretic behavior of nailed connections. At the elementary cell and shear wall scales, push-over and reversed-cycle tests are performed to obtain the hysteretic behavior as a function of infill characteristics. Walls without any openings (doors or windows) were considered. Through these tests, the influence of the infill on stiffness, maximum load or equivalent viscous damping is analyzed. The present work is then compared with three other experimental studies on the same type of traditional structures in order to provide answers regarding their seismic-resistant behavior.

Based on this experimental multi-scale analysis, this article confirms that the timbered masonry structures have a relevant seismic resistant behavior and provides a full analysis useful for the development of a numerical tool aiming at predicting the seismic resistant behavior of this kind of structure.

1. Introduction

According to Gurpinar et al. [1], existence of timber frame structures with infill are several millennia old, originating from the Neo-Hittite states (northern Syria and southern Turkey) where timber frame structures filled with adobe were already used. In Italy, during the Roman period, an archaeological site excavation, located in Herculaneum, revealed a building with two levels of wood frame structure with infill. This type of structure was listed under the name of *Craticii* or *Opus Craticium* by Vitruvius [2].

Fig. 1, inspired by the work of Caimi [3], shows the worldwide distribution of the main timber frame structures with infill and especially in seismic prone area. The list is not exhaustive. For instance, timbered masonry structures exists all over the Europe (*colombages* in France, *half-timbered* in England, *fachwerkbau* in Germany, *intelaiata* in Italy, etc.). Likewise, similar to that used to build houses type *Bahareque* called *taquezal* technique can be found in Central America [4,5].

This kind of structure is widely used on the planet mainly due to the reduced cost of its construction thanks to the easy access to the materials contained therein, for its aesthetic and/or search of increased resistance to the seismic hazard (cf. Dutu et al. [6]). Indeed, traditional timber frame constructions with infill exhibited a remarkable behavior in recent large earthquakes (Turkey in 1999, Greece in 2003, Kashmir 2005 and Haiti in 2010) during which they have often suffered little damage. In comparison, the seismic resistant behavior of new construction made of masonry blocks or concrete was generally bad or disastrous (Haiti 2010). This is due to the lack of a building code and standards for the design of structures, due to the fact that seismic forces are not considered in the design of most buildings, also due to the poor quality of construction and/or materials (cf. [7]). Indeed, building such a structure whose implementation meets building codes has a relatively high cost makes these modern construction techniques inaccessible to the majority of local populations [8–11].

These findings raise an issue surrounding the minimal importance given to local architecture by the scientific community as well as those responsible for reconstruction efforts. Recently, some research project have been conducted in order to enhance the seismic resistant behavior knowledge of this kind of traditional wood frame structures. Regarding the experimental works, these authors can be cited encompassing the scale of the connection to the scale of the shear wall:

* Corresponding author. Address: 3SR Laboratory, Domaine Universitaire, BP53, 38041 Grenoble Cedex 9, France. Tel.: +33 625471578.
E-mail address: florent.vieux.champagne@gmail.com (F. Vieux-Champagne).

http://dx.doi.org/10.1016/j.engstruct.2014.02.020
0141-0296/

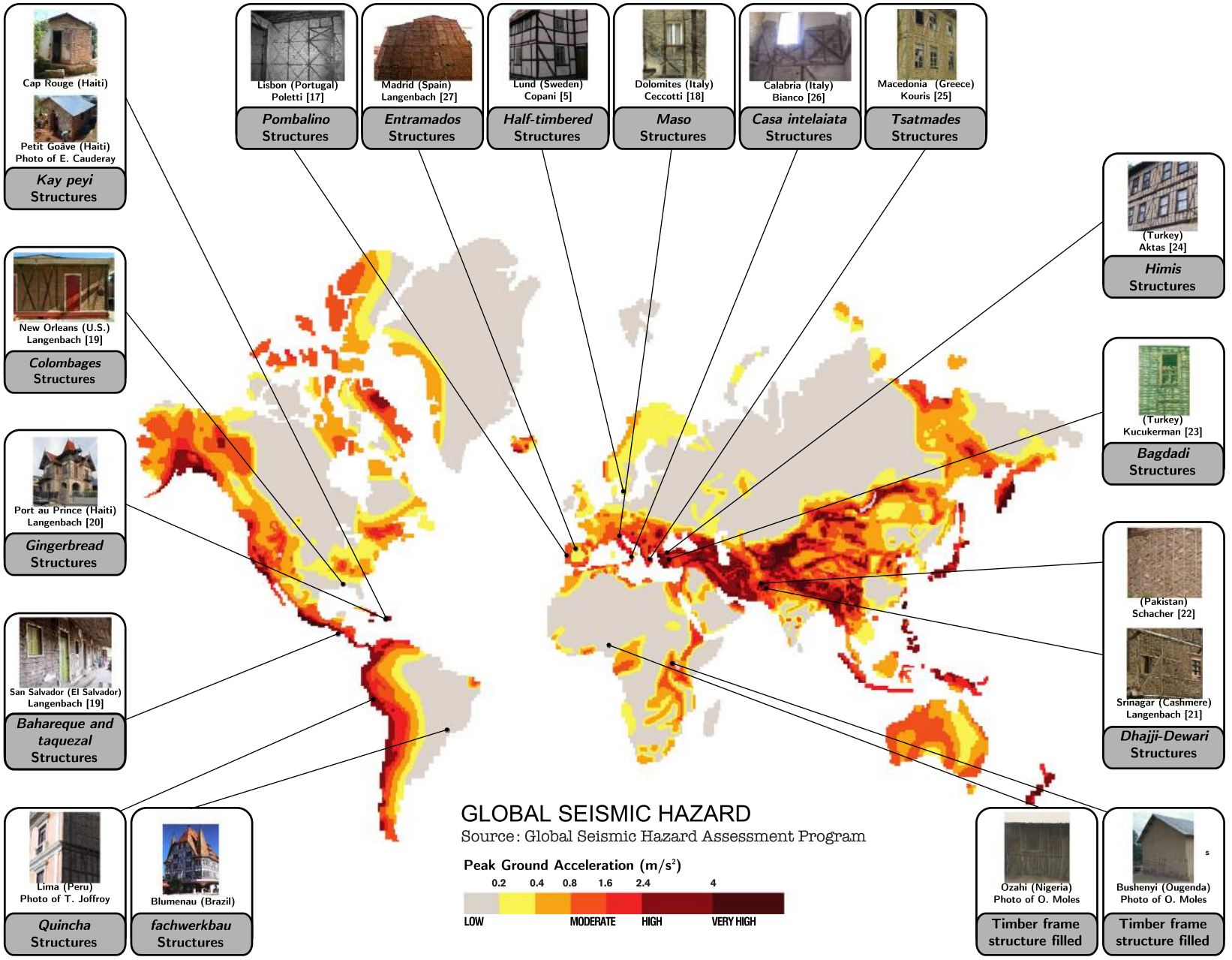

Fig. 1. Timber frame structures suitable with to the local constraints and potential ([5,17–27]), Base map: exhibition "Volcans, Séismes, tsunamis, vivre avec le risque" – Palais de la découverte (Paris) – October 12th 2007–May 11th 2008.

(a) Traditional (b) Built for a reconstruction project

Fig. 2. Rural Haitian houses.

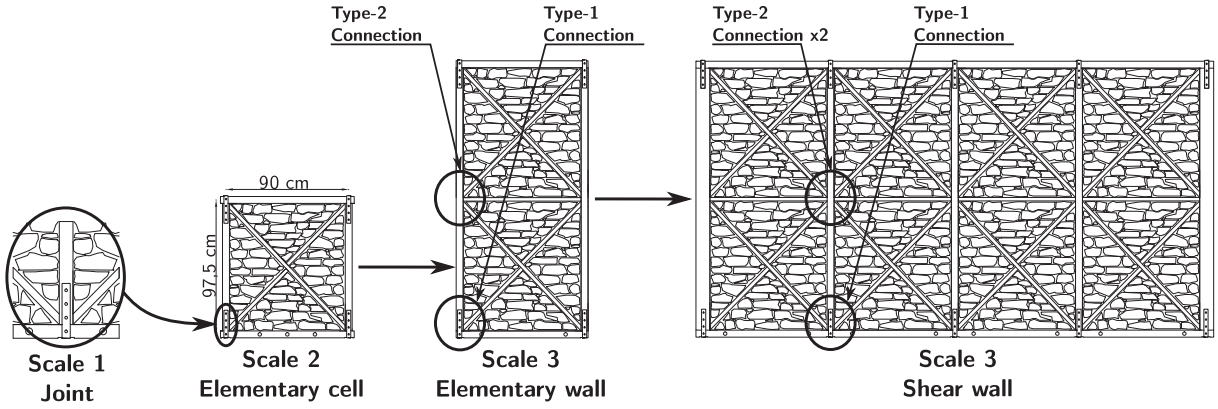

Fig. 3. The three scales of this experimental study.

- Connection: Ali et al. [12] (“Dhajji-Dewari” construction).
- Elementary cell: Ferreira et al. [13] (“Pombalino” construction).
- Reduced scale of a shear wall: Cruz et al. [14] (“Pombalino” construction) and Vasconcelos et al. [15] (“Pombalino” construction).
- Shear wall: Meireles et al. [16] (“Pombalino” construction), Poletti and Vasconcelos [17] (“Pombalino” construction), Ali et al. [12], Ceccotti et al. [18] (“Maso” construction).

All this shear tests are based on quasi-static loading and highlight a good seismic resistant behavior of these structures which are structurally quite different.

This paper presents the experimental study of a haitian timbered masonry structure called “Kay peyi” in an attempt to analyze its behavior under seismic loads and hence offer scientific answers regarding this set-up. This work is based on specific houses, as shown in Fig. 2, built via one of Haiti’s currently ongoing reconstruction projects.

This structure is studied at three scales, encompassing the connection (scale 1), the elementary cell (scale 2) and extending to the shear wall (scale 3). This multi-scale approach is illustrated in Fig. 3 and used in [38] for the seismic vulnerability analysis of timber frame structure using industrial products such as wood-products panels to braced the structure.

This approach provides an understanding of the behavior of the various wall components. At the first scale, type-1 connections are studied in order to determine the local influence of the nail number under two loading directions. The scale of the elementary cell then makes it possible to analyze the influence of the nature and presence of infill. Scale 3 (wall) is examined as a means of emphasizing the role of the type-2 connection, which does not exist at scale 2 and yields the global behavior of the structure.

This method also simplifies the study of the various elements described above and contributes experimental data for both a better understanding of the structural behavior and numerical investigations.

In the last part, the “Kay peyi” structure is then compared with three other experimental studies on the same type of traditional structures in order to analyze the structural differences

2. Description of the specimens and experimental set-up

2.1. Structure

Filled wood structures are built in many countries (including France, Germany, Italy, Pakistan, India and Haiti) (see Langenbach [19], Makarios and Demosthenous [9] and Dogangun et al. [28]) because of the fact that they use natural materials available on-site in most cases. This solution therefore is environmentally friendly (a key concern in developed countries) while being easier to build and less expensive (which receives considerable attention in emerging countries).

Three main types of such structures are prevalent in Haitian rural reconstruction projects: (1) bracing by San Andrew’s crosses (X-cross), filled with natural stones and bonded by an earth mortar (see Fig. 2); (2) bracing with just one diagonal and filled with adobes (handmade earth brick); and (3) braced by Wattle and daub

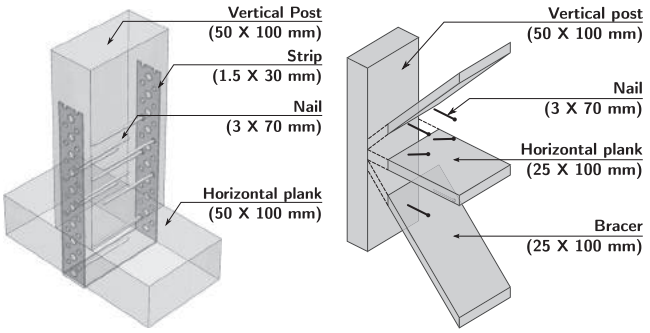

(a) Type-1 joint (b) Type-2 joint

Fig. 4. Nails connections of the timber structure.

(W & D) panels (with a frame made of pieces of wood or bamboo) and filled by earth mortar. The X-cross wall filled with stones has been selected for this study by virtue of being easiest to build and thus the most widespread. The X-crosses simplify filling of the structure and enhance safety in the case of falling stones thanks to smaller-sized infill parts. Large pieces of wood however are more difficult to procure by the local population.

The earth is composed of a 1/1 ratio of a clay-calcareous mix ($D < 125$ μm), a 2/1 ratio of sand ($D < 2$ mm), a 1/2 ratio of water (depending on the water content of sand) and a 1/1 ratio (very coarse measure) of sisal fibers (easily available in Haiti). To prevent the mortar from cracking, the water content must be limited in the earth and moreover sisal fibers are to be added. The clay-calcareous mix is chosen to obtain a mortar as close as possible to what can be produced from the local earth.

The fibers serve to limit the appearance of cracking and its propagation in mortar. Plain shank nails (also called "common nail") are thus placed inside wood triangles to improve the bond between both parts (see Fig. 8(b)).

The bracings are made from Saint Andrew's crosses with one continuous diagonal and another diagonal divided into two parts (Fig. 3). They are connected to the vertical post using two 70-mm long plain shank nails (Fig. 4(b)). These techniques facilitate construction and avoid weakening the wood in comparison with an edge half lap joint located at the center of each diagonal.

Various connections are used to build the structure described above (see Fig. 4) though not all exert the same influence on the seismic resistance of the structure. In this study, only the connection with the greatest impact on wall behavior has been tested at scale 1, *i.e.* a steel-wood nailed connection (Fig. 4(a)) consisting of a punched steel strip surrounding the wood parts (in a T-shape) and fastened by a few nails that govern behavior of the connection. The timber strength class is C18 with a density $\rho_{mean,C18} = 380\ \mathrm{kg/m^3}$ according to European standard EN 338 (see EN 338 [29]). The strip is a FP30/1, 5/50 from Simpson Strong-Tie®, 30 mm wide and 1,5 mm thick. 3×70 mm plain shank nails are used (see EN 10230-1 [30]) to fasten the strip.

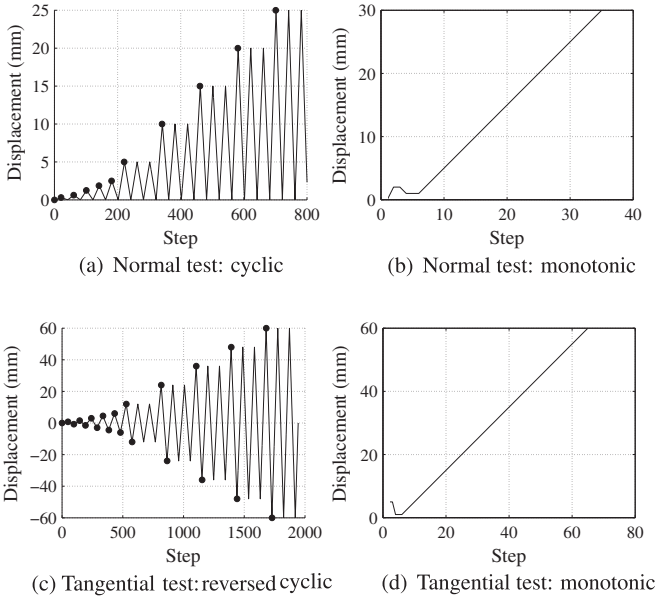

Fig. 6. Loading protocol.

2.2. Experimental set-up

2.2.1. Scale 1: Connections

Normal (vertical) and tangential (horizontal) tests have been conducted on these connections, as shown in Fig. 5, to generate the force-displacement response in both directions. As regards the third direction of connection behavior, *i.e.* the moment-rotation law, this was not studied due to its very low resistance compared to the other two directions.

(a) Normal test (b) Tangential test

Fig. 5. Tests on the connections.

Table 1
Configuration of the normal and tangential tests conducted on joints.

Type of tests	Number of nails per connection
3 monotonic 1 cyclic	$\{1-2-3-4\} \times 2$

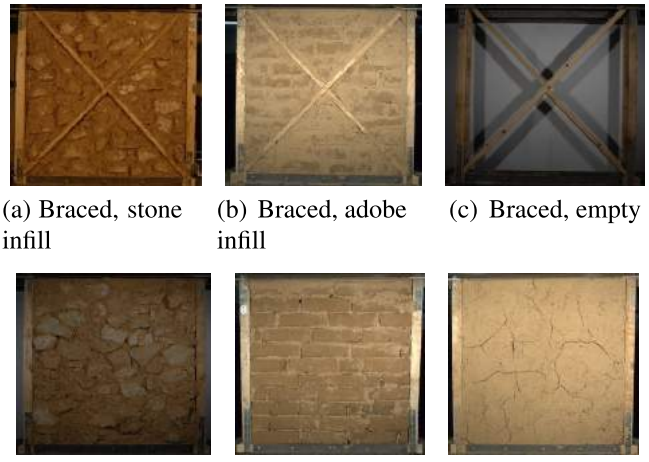

(a) Braced, stone infill (b) Braced, adobe infill (c) Braced, empty

(d) Unbraced, stone infill (e) Unbraced, adobe infill (f) Unbraced, wattle & daub infill

Fig. 7. Elementary cell tested.

Table 2
Elementary cell test configurations.

Bracing	Type of tests	Infill
X-cross	1 monotonic 2 cyclic	Stone
X-cross	1 monotonic 4 cyclic	Adobe
X-cross	1 monotonic 2 cyclic	Empty
None	1 cylic	Stone
None	1 cylic	Adobe
None	1 cylic	W & D
None	1 cylic	Empty

Table 1 lists the characteristics of the normal and tangential tests carried out on joints. The loading path was adjusted to take into account the ISO/FDIS 21581:2010(E) standards (timber structures – static and cyclic lateral load methods for shear walls, see ISO 21581 [31]). The shape of the loading history is provided in Fig. 6. These tests are displacement-controlled with displacements being measured by means of linear variable differential transformer (LVDT) at a rate that depends on cycle displacement (30 s between two consecutive peaks). The maximum speed reached during testing equals 1 mm/s. For each test protocol, 2, 4, 6 and 8 nail joints (with the same number of nails on both sides) were evaluated according to three monotonic tests, one cyclic test (for the normal direction shown in Fig. 6(a)) reversed cyclic test (for the tangential direction displayed in Fig. 6(c)).

2.2.2. Scale 2: Elementary cell

As previously explained in Section 2.1, rural Haitian houses are built according to different techniques. Their behavior under seismic loading can obviously differ from the test case behavior. A good design requires an evaluation of these differences. It is quite complicated however to modify many parameters over an entire wall. A testing apparatus, shown in Fig. 8(a) has thus been designed to test an intermediate scale, such as an elementary cell, that remains part of the wall.

The three types of infill used in Haiti along with the empty configuration have been tested. To assess the influence of bracings and filling, a number of tests were then performed on three configurations without diagonal members and with different infill.

Table 3
Elementary wall test configurations.

Type of tests	Infill
1 monotonic 1 cyclic	Stone
1 monotonic 1 cyclic	Empty

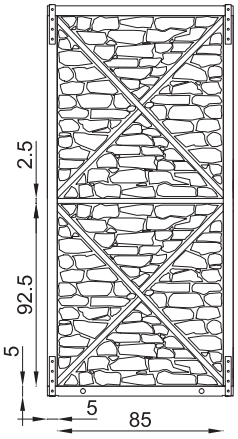

Fig. 9. Elementary wall dimensions.

All the configurations tested are presented in Fig. 7 and Table 2. The cell dimensions and building techniques are illustrated in Fig. 8(b).

On both top sides of the elementary cell, rollers apply the loading through a steel plate fastened onto wood. These rollers prevent against parasite moment transmission, while the steel plate distributes the horizontal load in both the horizontal beam and vertical post. The bottom of the horizontal wood bar is anchored on the steel horizontal reaction beam using eight bolts. The loading program is the same as that depicted in Fig. 6(c) with an 80 mm maximum displacement. All tests are displacement-controlled at a rate of $2,2$ mm/s.

For each braced configuration, two reversed cyclic tests and one monotonic test have been performed, except for the adobe configuration, which features four cyclic tests. In this case, two additional configurations (Cyclic 3* and Cyclic 4*) were tested in order to investigate specific technical detail variations, such as making an X-cross with an edge half lap joint at the middle of the diagonal and changing the contact between the end of the X-cross and the timber frame (with diagonals being fastened to the horizontal wood beam instead of the vertical post).

2.2.3. Scale 3: Shear wall

A wall is compounded by two elementary cells in vertical direction and *n* elementary cells in horizontal direction. Scale 3

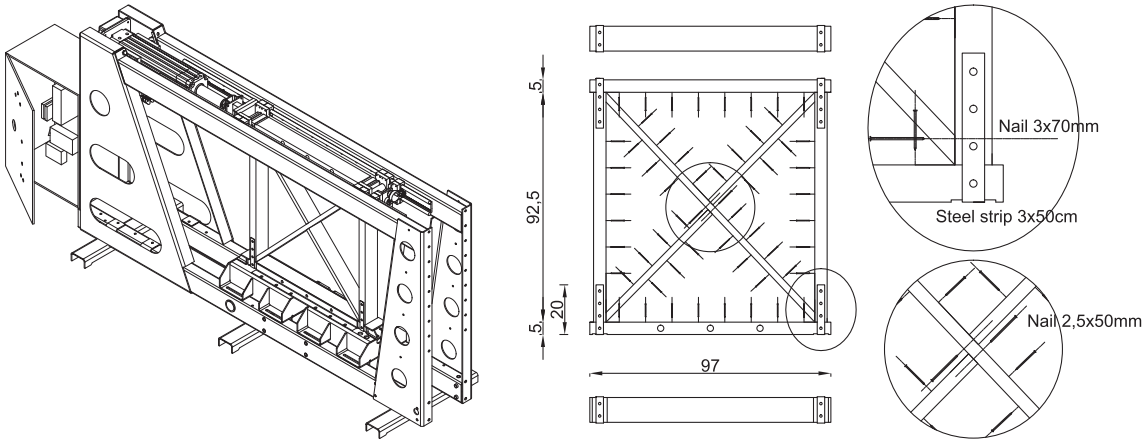

(a) shear test on an elementary cell (b) elementary cell dimensions

Fig. 8. Elementary cell layout.

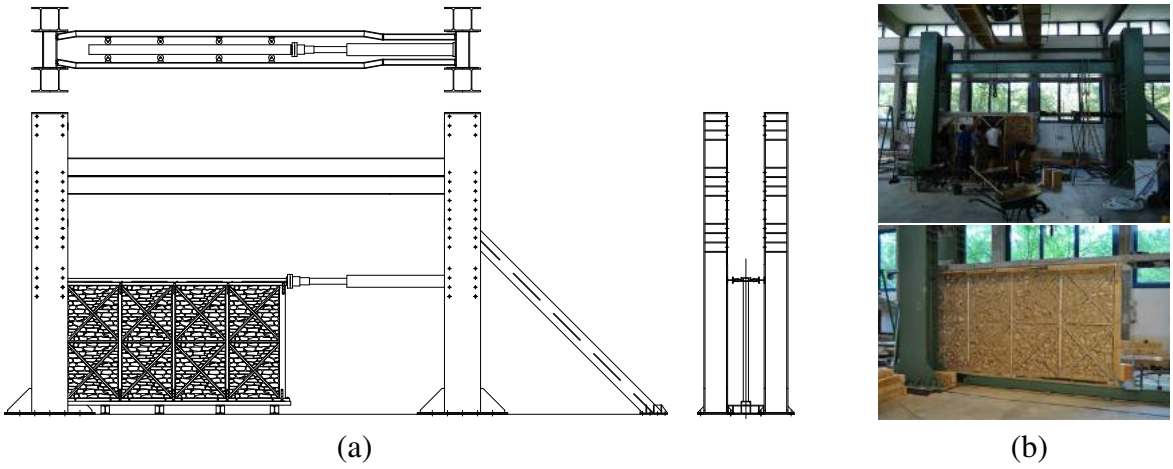

Fig. 10. The scale of the wall.

Table 4
Wall test configurations.

Type of tests	Infill
1 monotonic 2 cyclic	Stone
1 monotonic 1 cyclic	Empty

emphasizes the role of the type-2 connection, which does not exist at scale 2 and yields the global behavior of the structure.

2.2.3.1. Elementary wall, $n = 1$. First, a specific case of the shear wall was studied ($n = 1$). It is relevant since it integrates the type-2 connection and remains straightforward to set up in comparison with the entire wall. Table 3 presents the test-related characteristics. Compared to scale 2, tests on the elementary wall highlight the influence of infill on the behavior of the structure. The dimensions of the scale 3 framework are provided in Fig. 9.

The loading path of the elementary wall test is exactly the same as that of the elementary cell.

2.2.3.2. Shear wall, $n = 4$. The experimental program has been carried out at the Mechanical Testing Laboratory of CNR IVALSA in Trento (Italy). The filled walls were built directly on the testing apparatus due to the difficulty involved in moving them (see Fig. 10). After construction, the wall was therefore covered with a plastic tarpaulin and a dehumidifier introduced to accelerate drying of the earth mortar ($h = 30\%$, $T = 20$–25 °C). As a result, the mortar dried in just three days.

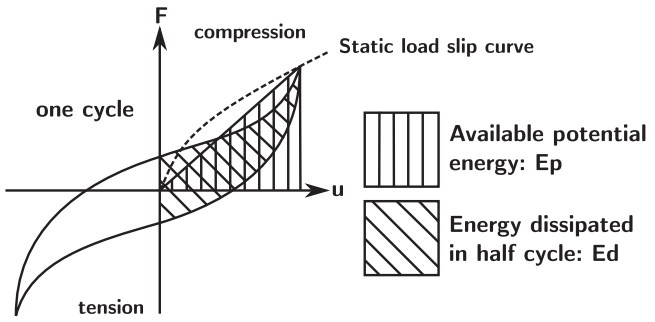

Fig. 11. Definition of E_d and E_p in determining the equivalent viscous damping ratio for one cycle, see EN 12512 [32].

The wood characteristics and dimensions are identical to those of the elementary wall, except for the end posts, which have a 100×100 mm cross section.

Moreover, the loading path is the same as that applied to the elementary cell and the tests are still displacement-controlled. The wall is embedded using the same method as for the elementary cell. To prevent buckling, hard rubber casters maintain the top wood beam of the wall. The roofs on Haitian houses are built with sheet metal. These roofs are therefore very lightweight and for this reason, no vertical load is applied on the wall. Table 4 presents the configurations applicable to the wall test.

3. Results

This part of the paper will present the results of tests extending from scale 1 to scale 3. For each case, the load–displacement or load–drift curves are given along with the main numerical values summarized in a table. The drift ratio refers to the ratio of top lateral displacement to wall height and is expressed as a percentage. This drift value allows comparing structures at various heights.

From scale 2 to scale 3 for the purpose of assessing the energy dissipation capacity of these structures, the equivalent viscous

Table 5
PS nailed connection: normal tests results.

Number of nails (n)	Loading (–)	F_{max} (kN)	$F_{max}(n)/n$ (kN)	d_{max} (mm)
1×2	Monotonic	2.6	1.3	3.7
	Monotonic	2.2	1.1	7.1
	Monotonic	2.3	1.2	5.1
	Cyclic	2.3	1.2	6.0
2×2	Monotonic	4.8	1.2	7.9
	Monotonic	5.4	1.4	6.9
	Monotonic	5.6	1.4	7.9
	Cyclic	5.5	1.3	9.3
3×2	Monotonic	7.9	1.3	8.8
	Monotonic	8.7	1.5	9.4
	Monotonic	7.0	1.2	8.4
	Cyclic	7.5	1.3	9.2
4×2	Monotonic	11.2	1.4	9.8
	Monotonic	10.7	1.4	11.0
	Monotonic	10.0	1.3	11.4
	Cyclic	9.2	1.2	10.6
$\overline{F_{max}(n)/n}$	–	–	1.3	–
σ_d	–	–	0.1	–

Table 6
PS nailed connection: tangential tests results.

Number of nails (n)	Loading (–)	F_{max} (kN)	$F_{max}(n)/n$ (kN)	d_{max} (mm)
1	Monotonic	2.1	2.1	29.7
	Monotonic	2.4	2.4	40.8
	Monotonic	2.0	2.0	27.3
	Cyclic	2.2	2.2	36.2
2	Monotonic	3.3	1.7	34.7
	Monotonic	2.6	1.3	42.9
	Monotonic	3.4	1.7	44.1
	Cyclic	2.9	1.5	24.1
3	Monotonic	4.5	1.5	42.8
	Monotonic	3.9	1.3	32.5
	Monotonic	3.5	1.2	34.3
	Cyclic	3.4	1.1	24.2
4	Monotonic	5.0	1.3	48.9
	Monotonic	4.0	1.0	59.0
	Monotonic	4.0	1.0	49.5
	Cyclic	4.3	1.1	36.1

damping (EVD) has been calculated from the force-deformation hysteresis loops (see Fig. 11) by applying Eq. (1) (EN 12512 [32]).

$$\xi_{eq} = \frac{E_d}{2\pi \cdot E_p} \tag{1}$$

where E_d is the dissipated energy, which equals the area of the hysteresis loop, and E_p is the elastic energy, equal to half the product of the maximum force and the corresponding displacement.

The mean value ξ calculated for both positive and negative drift is then given for each test.

3.1. Scale 1: Connections

The results of normal and tangential tests on joints can be observed in Fig. 12 and are summarized in Tables 5 and 6. For each configuration (from two to eight nails), Fig. 12(a) shows the average curve (A) of all three monotonic tests (*e.g.* A 2) and the envelope curve (Env) (*e.g.* Env 2) of the associated cyclic test. The number following the letter indicates the number of nails. Tables 5 and 6 summarize, for each test, the maximum load reached and its corresponding displacement. They also provide the maximum load reached per nail. These tables along with Fig. 12(b) demonstrate that for a normal test, $F_{max}(n)/n$ is nearly constant with an average value equal to 1.3 kN and a low standard deviation $\sigma_d = 0.1$ kN. These results suggest that the maximum load is proportional to the number of nails and moreover are consistent with the results derived by Fonseca et al. [33] (test no. 44), which yields an average maximum load per nail of 1 kN. On the other hand, for tangential tests, $F_{max}(n)/n$ decreases as the number of nails increases.

In order to obtain these results, the density ρ of the wood has been taken into account since it exerts a significant impact on joint strength and varies greatly within the same timber strength class (see Dorn et al. [34]). As an example, for the 32 configurations studied, the average density $\bar{\rho}$ is equal to 412 kg/m^3 and the standard deviation is 49 kg/m^3. In the connection section of EN 1995-1-1 [35], the embedment strength $f_{h,k}$ (N/mm^2) without predrilled holes is given by the expression in Eq. (2).

$$f_{h,k} = 0.082 \cdot \rho_k \cdot d^{-0.3} \tag{2}$$

where d is the nominal diameter of the nail, in mm.

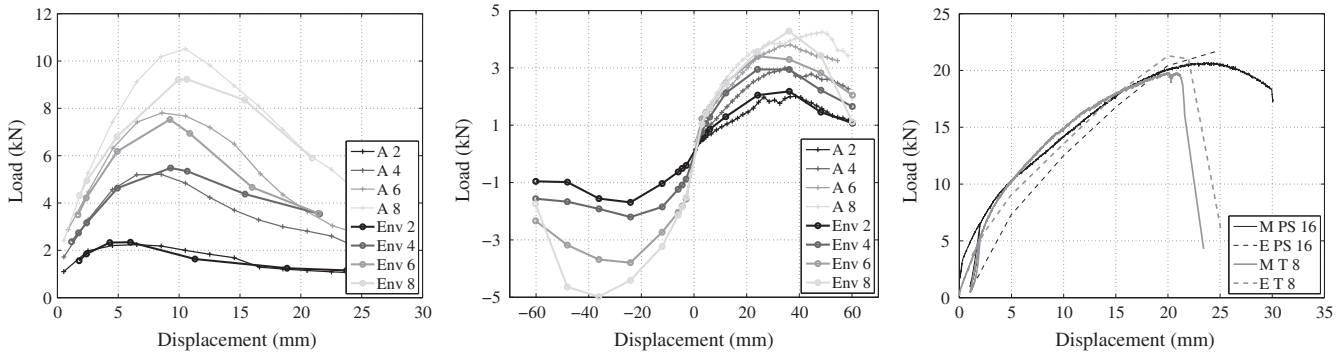

(a) Normal test results (b) tangential test results (c) Threaded nails vs plain shank nails

Fig. 12. Load–displacement diagram – connections.

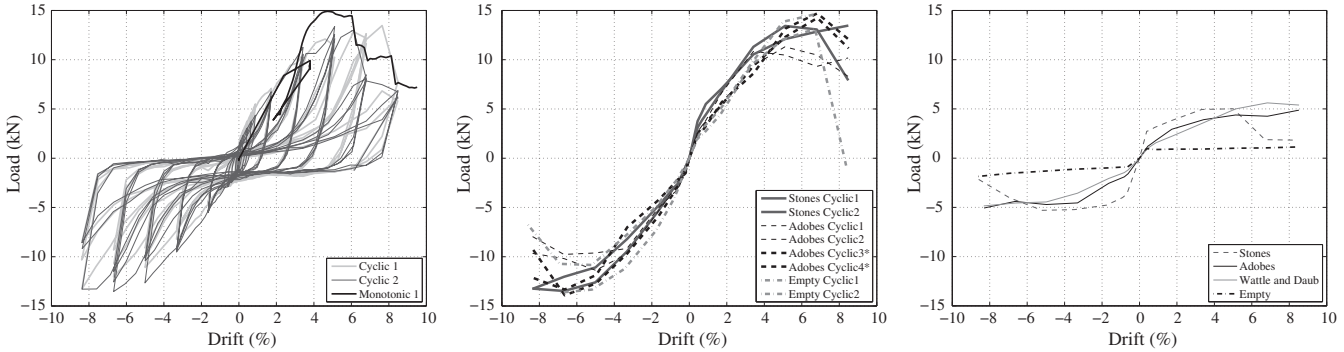

(a) Cyclic curves for braced cells filled with stones (b) Cyclic enveloped curves for braced cells (c) Cyclic enveloped curves for unbraced cells

Fig. 13. Load–drift diagram – elementary cell.

Table 7
Shear test results on elementary cells.

Type of infill (–)	Loading (–)	$F_{min/max}$ (kN)	$\text{drift}_{min/max}$ (%)	ξ (%)
Stones	Cyclic1	−12.6/12.8	−7.95/8.06	11.8
	Cyclic2	−12.8/12.8	−6.35/4.85	12.7
	Monotonic	–/14.3	–/4.48	–
Adobes	Cyclic1	−9.1/10.2	−6.35/3.25	13.8
	Cyclic2	−10.7/10.7	−4.75/4.85	13.1
	Cyclic3*	−12.7/14.1	−6.32/6.49	12.0
	Cyclic4*	−13.3/13.6	−6.31/6.49	12.8
	Monotonic	−12.9/–	−4.47/–	–
Empty	Cyclic1	−13.0/14.0	−6.55/6.37	10.6
	Cyclic2	−10.2/12.5	−4.94/6.37	11.5
	Monotonic	−12.0/–	−4.83/–	–
$\overline{F_{max}}$		−11.9/12.8	−5.88/5.69	
σ_d		−1.4/1.4	−1.04/1.36	

Table 8
Shear test results on unbraced elementary cells.

Type of infill (–)	$F_{min/max}$ (kN)	$\text{drift}_{min/max}$ (%)	ξ (%)
Stones	−4.9/4.9	−4.73/3.26	16.8
Adobe	−4.5/4.3	−7.89/8.09	17.1
W & D	−4.3/5.0	−7.90/6.49	13.4
Empty	−1.3/0.5	−8.17/7.94	–

As the number of test is not important and that objectives are not to design the joints according to Eurocode prescriptions, mean values are used herein.

By dividing the experimental embedment strength f_h by the theoretical strength value of C18 wood, it becomes possible to weight the load F, as given by Eq. (3).

$$F_{C18} = \frac{\rho_{mean,C18}}{\rho} \cdot F \tag{3}$$

where F_{C18} is the load corresponding to the embedment strength, as calculated using the average density of the C18 timber, $\rho_{mean,C18}$.

For the tangential test results, this method is irrelevant since no substantial variation was observed. In contrast, the normal test results are obviously of benefit to the analysis.

Complementary tests have been conducted with a threaded nail (T) connection, which happens to be more widely used in more developed countries. Fig. 12(c) compares the load–displacement diagram for one cyclic (envelop curve (E)) test and one monotonic (M) normal test derived for an 8 T nailed connection and a 16 plain shank nail (PS) connection. These results are suitable for comparison since the maximum load and corresponding displacement are approximately the same for both configurations. The T nailed connections prove to be more resistant than the PS nailed connection, in addition to yielding a more brittle behavior. For the former configuration, the strip failed whereas plain shank nails can pull out and prevent the strip from failing. Furthermore, T nails are far more expensive; it is therefore preferable to use PS nails with a low pull-out risk in the connection.

3.2. Scale 2: Elementary cell

Fig. 13(a) shows the load–drift diagram for the tests conducted on stone-filled cells. A certain pinching behavior can be observed. A technical incident occurred during the monotonic test that led to a linear curve until 25 mm displacement as well as an abnormal loop. Fig. 13(b) and (c) illustrate the load–drift ratio diagram for both braced and unbraced elementary cells subjected to reversed cyclic (C) and monotonic loading (M) tests. Results are summarized in Tables 7 and 8.

(a) Connection failure during a cyclic test (b) Connection failure during a monotonic test (c) Connection out of plane failure

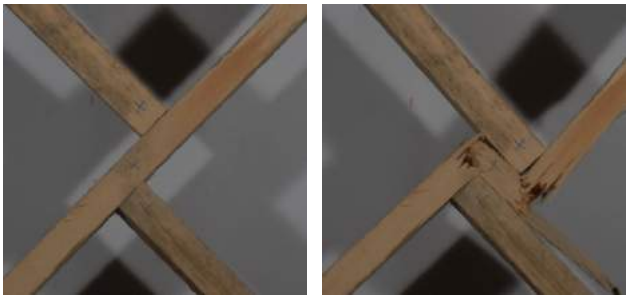

(d) Bracing (e) Failure of the bracing

Fig. 14. Failure modes.

Fig. 13(b) compares three types of X-cross braced cells: (1) filled with stones, (2) filled with adobes, and (3) empty. The filled configurations (Stones 1 and 2 and Adobes 1–4), in comparison with the empty configurations (Empty 1 and 2), reveal that infill has little influence on cell behavior. Likewise, Adobes 1 and 2, when contrasted with Adobes 3* and 4*, indicate that technical specifications on the bracings also exert little influence on their behavior (see Section 2.1).

As a matter of fact, the average maximum load is very close for each configuration:

- Stones (S) infill: $\overline{F_{max}} = 13.9$ kN, $\sigma_d = 0.7$ kN.
- Adobes (A) infill: $\overline{F_{max}} = 12.9$ kN, $\sigma_d = 1.6$ kN.
- Empty (E): $\overline{F_{max}} = 13.2$ kN, $\sigma_d = 1.1$ kN.

This result is due to the fact that the cell behaves like a lattice and hence the infill has only two effects: it prevents the bracing from failure, as seen in Fig. 14(e), and it modifies the stiffness (see Fig. 13(b)).

The lower strength of the Adobe 1 and Adobe 2 configurations are due respectively to the out-of-plane failure of the connections shown in Fig. 14(c) and to the inadequate distance between two consecutive nails and the edge of the post. In the first case, the strip is bent under the horizontal loading of the out-of-plane bracing. For both of these cases, the consequences are an early pull-out of the nail.

Under monotonic tests, cells exhibit a more brittle behavior. This stems from the uniaxial loading of the connection (normal direction), as observed in Fig. 14(b). In contrast, during a cyclic test, the connections are loaded in the normal and tangential directions (Fig. 14(a)) thereby increasing overall cell ductility. Regarding the E M 1 test, the distance between the wood half-diagonals at the cell center was too great and therefore broke at a small displacement. For filled configurations, this parameter is considered less critical since the infill prevents excessive wood deformation.

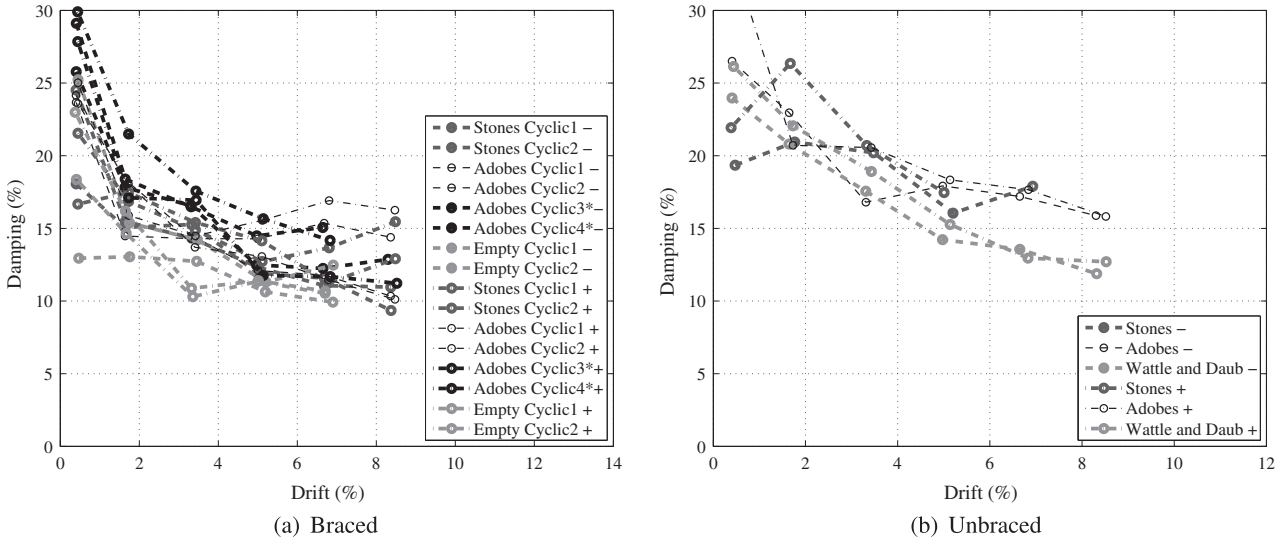

(a) Braced (b) Unbraced

Fig. 15. Damping–drift diagram for cells in the first loop of each yield displacement.

Comparison between Fig. 13(b) and (c) shows the influence of the X-cross in the cell. Without this structural element, the maximum load is less than half the X-cross cell value caused by low infill strength. This comparison also indicates that the type of infill used to test the cell exerts no influence on its lateral load capacity, but more on initial stiffness. Furthermore, the empty cell has a residual strength of approximately ±0.4 kN. It confirms that the moment-rotation law for the connection is insignificant regarding both the normal and the tangential directions.

Fig. 15 depicts the comparative trend between damping ratio and drift for both the braced and unbraced cells. In order to improve the legibility of these graphs, only the cycle loop with a bullet point has been plotted (see Fig. 6ch configuration, (+) and (−) signs have been represented in the same direction on these graphs. It appears that damping is high for the first cycles then decreases during the subsequent cycles because the load at 0 displacement is high compared to the maximum cycle load that leads to a high E_d value and consequently a high value of ξ_{eq} in accordance with Eq. (1). As shown in Fig. 15(a), this ratio tends towards a constant value of around 12.5% (see Filiatrault et al. [36]) which is consistent with wood construction and represents a favorable condition for the structure subjected to seismic loading. As explained above, ξ is a mean value calculated for both a positive and negative drift >|4%|, given that from this value forward, it remains constant. Experimental variability is obviously substantial across an array of configurations, as well as between positive and negative drifts for the same configuration. Fig. 15(a) and Table 7 apparently show that the damping ratio of filled cells is higher than that of empty cells, thus reinforcing the observations listed in Ali et al. [12]: masonry infill does not contribute to lateral load capacity, but does increase the energy dissipation capacity of the system. Fig. 15(b) and Table 8 reveal that the infill of unbraced cells, despite its low lateral load capacity, dissipates a reasonable amount of energy since the damping ratio is equal to approximately 17% for stone and adobe. For Wattle and daub, ξ is only equal to 13.4% since it is composed of a mesh of intertwined branches covered by mud and hence less able to dissipate energy.

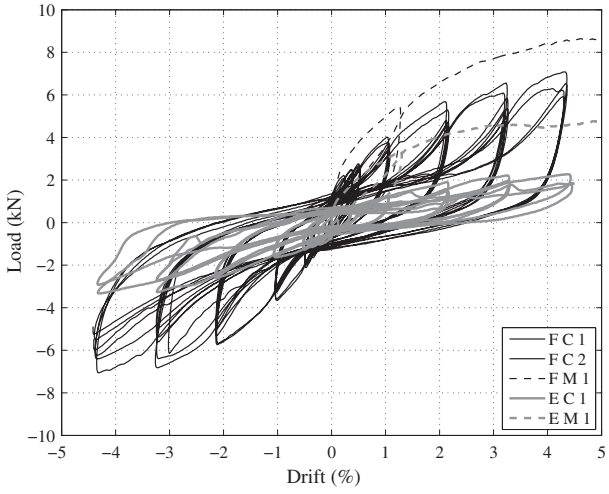

Fig. 16. Load–drift diagram – elementary wall both filled and empty.

Table 9
Elementary wall test results.

Type of wall (–)	Loading (–)	$F_{min/max}$ (kN)	$drift_{min/max}$ (%)	ξ (%)
Filled	Cyclic1	−7.1/7.1	−3.88/3.86	13.6
	Cyclic2	−6.4/6.3	−2.89/3.68	14.2
	Monotonic	–/8.6	–/4.04	–
Empty	Cyclic	−3.4/2.2	−3.84/3.90	16.5
	Monotonic	–/5.5	–/7.23	–

3.3. Scale 3: Shear wall

3.3.1. Elementary wall, $n = 1$

Fig. 16 presents the load–drift diagram for reversed cyclic (C) and monotonic (M) tests on both filled (F) and empty (E) elementary walls. The main values are summarized in Table 9. This diagram shows the significant effect of infill on wall behavior: the maximum load is more than twice for a filled configuration than an empty one.

In light of Fig. 17(a) and (b), flexural deformation in the bottom left post is more pronounced for the empty wall. This finding can be explained by limiting deformations with infill, hence a global rigid rotation on the left type-1 connection with a move upward on the right type-1 connection (Fig. 17(c)). On the other hand, the timber frame is free to bend for the empty wall and the type-

(a) Filled elementary wall deformation at the end of the cyclic test

(b) Empty elementary wall deformation at the end of the cyclic test

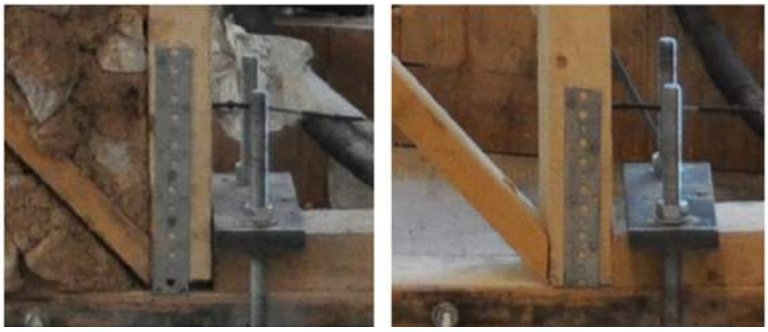

(c) Connection damage for the filled structure at the end of the cyclic test

(d) Connection of the empty structure at the end of the cyclic test

Fig. 17. Deformation of a filled elementary wall.

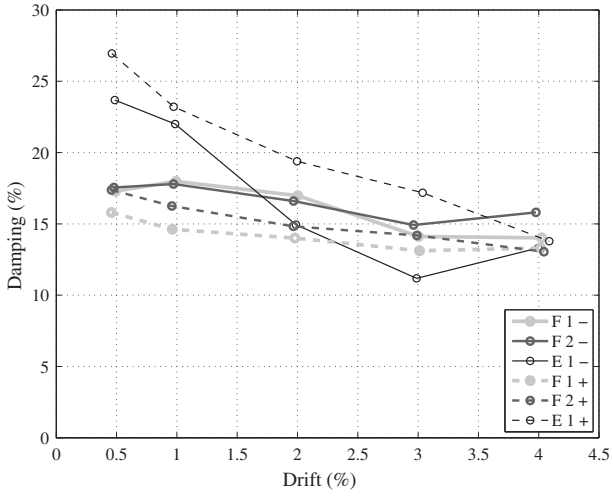

Fig. 18. Damping–drift diagram – elementary wall both filled and empty.

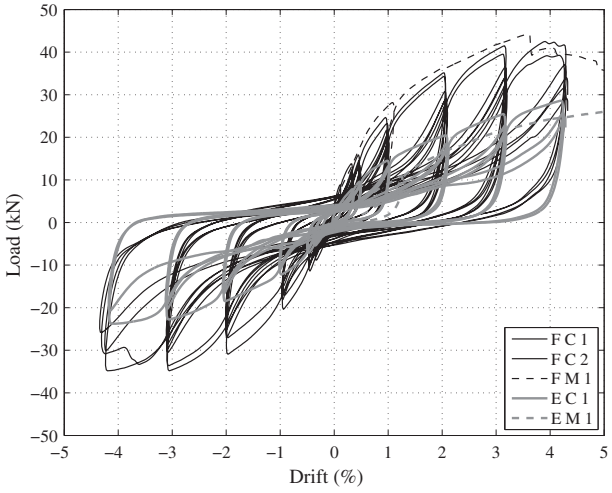

Fig. 19. Load–drift diagram – wall both filled and empty.

1 connection is undamaged (Fig. 17(d)) which explains the higher strength of the filled structure.

As shown in the damping–drift diagram for the elementary wall (see Fig. 18), the equivalent viscous damping is nearly constant and approximately equal to 15%. As presented above, this value is consistent for wood construction and remains appropriate for a seismic-resistant structure.

3.3.2. Shear wall, n = 4

Fig. 19 depicts the load–drift ratio diagram for filled (F) and empty (E) shear walls under cyclic (C) and monotonic (M) loading. The main values are summarized in Table 10.

Table 10
Shear wall test results.

Type of wall (–)	Loading (–)	$F_{min/max}$ (kN)	$drift_{min/max}$ (%)	ξ (%)
Filled	Cyclic1	−33.6/42.5	−2.75/3.52	15.3
	Cyclic2	−34.8/39.5	−2.75/2.8	15.4
	Monotonic	–/44.3	–/3.26	–
Empty	Cyclic	−23.8/28.6	−3.65/3.78	17.2
	Monotonic	–/26.9	–/5.21	–

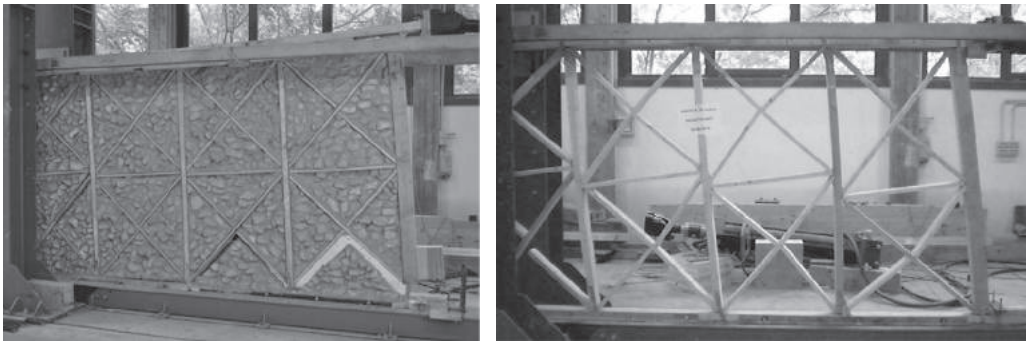

(a) Filled wall deformation at the end of the monotonic test (b) Empty wall deformation at the end of the monotonic test

Fig. 20. Deformation of a filled wall.

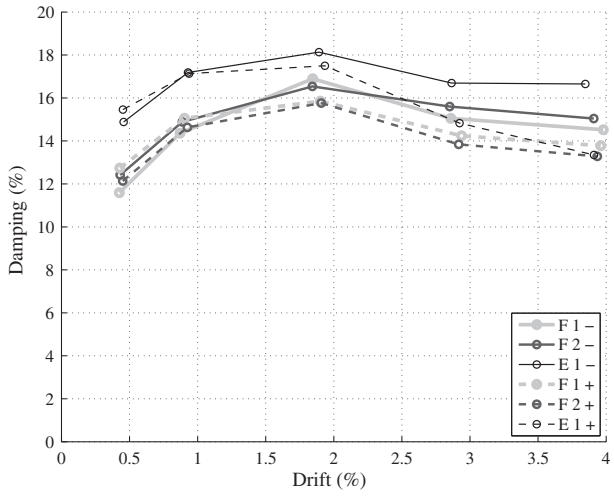

Fig. 21. Damping–drift diagram – wall both filled and empty.

Unlike the results on cells, Fig. 19 shows that for the wall infill has a significant influence on both initial stiffness and lateral load capacity. The cells actually behave like a lattice, leaving the infill unsolicited, whereas in the empty wall, the type-2 connections between the X-crosses exhibit large displacement (see Fig. 20(b)), which allows for deformation of the timber frame without loading the type-1 connections. In contrast, infill limits this deformation and makes the wood structure deform almost like a lattice. Deformations are thus mainly concentrated in the nail-strip connections (see Fig. 20(a)).

Fig. 19 also shows the significant pinching effect on these shear walls, which becomes marked for timber structures under seismic loading. Each sudden loss of resistance during the F M 1 test (visible for a drift of $3,5\%$) and the F C 1 test (visible for a drift of 4%, see Fig. 19) is due to a nail head failure. This phenomenon appears to be major since it causes a more brittle global wall behavior.

As shown in the damping–drift diagram for the elementary wall, the equivalent viscous damping is nearly constant and approximately equal to 15% (see Fig. 21). The ξ value for an empty wall is slightly higher than for a filled structure, which confirms that the main impact of infill is to make the timber structure behave like a lattice. It can be assumed that the dissipation energy is almost exclusively due to the deformation of joints and not to infill damage.

4. Comparison of traditional structures

The framework studied in this paper will be named “kay peyi” (name given for this kind of structure in Haiti) in this section in order to simplify comparisons.

Previously presented results will now be compared with three other experimental works on the same kinds of structural frames: Pombalino (Portugal), Dhajji-Dewari (Pakistan), and Maso (Italy).

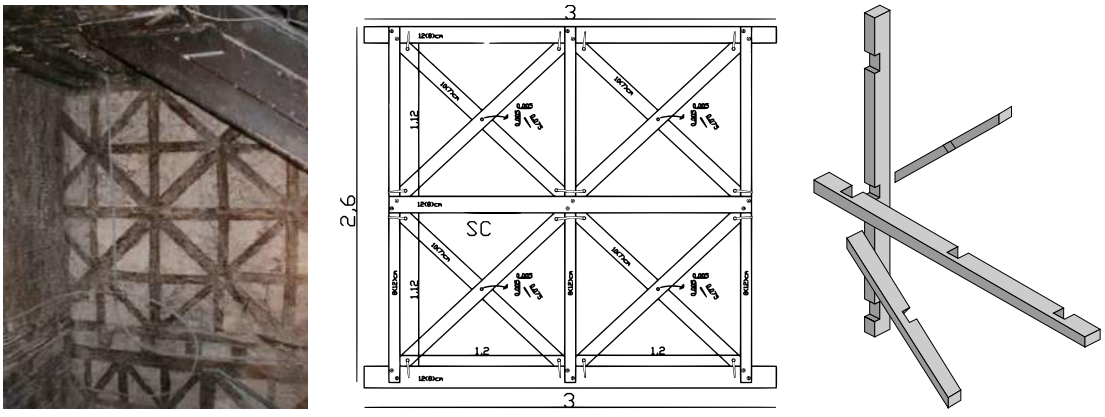

(a) *in situ* wall (b) The wall tested (filled) (c) The wall connection

Fig. 22. “Pombalino” frontal wall (pictures extracted from Meireles et al. [16]).

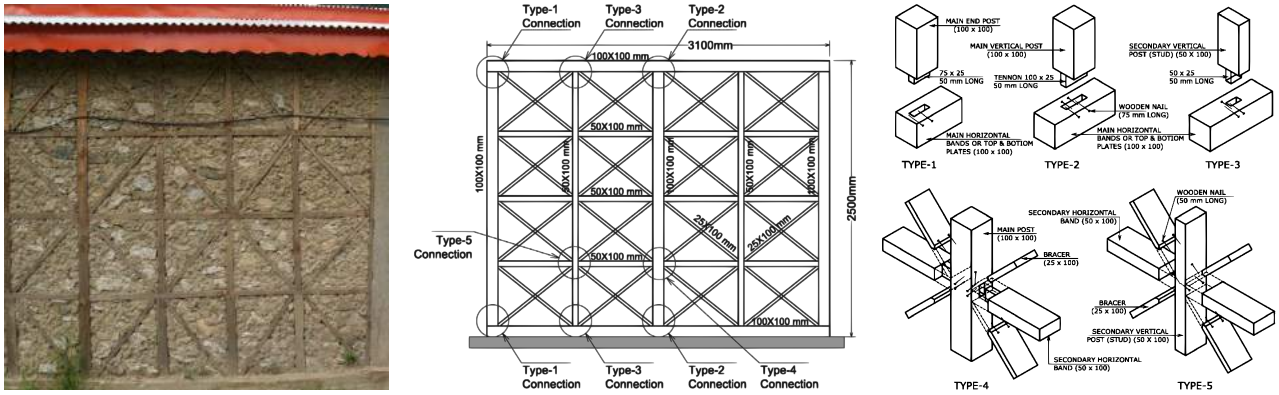

(a) *in situ* wall (b) The wall tested (filled) (c) The wall connection

Fig. 23. "Dhajji-dewari" wall (pictures extracted from Ali et al. [12]).

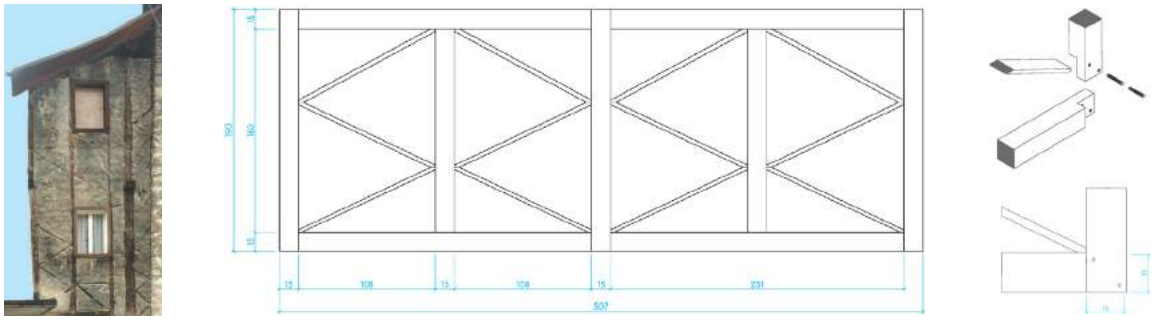

(a) *in situ* wall (b) The wall tested (filled) (c) The wall connection

Fig. 24. "Maso" wall (pictures extracted from Ceccotti et al. [37]).

Table 11
Test comparison – filled walls – general values and observations.

Wall tested (–)	Dimensions (m^2)	Vertical loading (kN)	Type of joint (kN)	$\|F_{max}\|$ (%)	$Drift_{F_{max}}$ (%)	ξ	Failure location (–)
Kay peyi	3.6×2.0	0	Steel strip	42.5	3.0	15.3	Joint
Pombalino [16]	3.0×2.6	90	LJ[a], CHJ[b]	50.0	2.3	19.5	CHJ
Dhajji-Dewari [12]	3.1×2.5	6	M&T[c]	13.7	2.5	15.0	Joint
Maso [37]	5.1×1.9	$\propto$ HL[d]	LJ screwed	74.4	2.1	18	Bracing

[a] Lap Joint.
[b] Cross Half Lap Joint.
[c] Mortise and tenon nailed.
[d] Horizontal Load.

Table 12
Test comparison – filled walls – influence of the infill.

Wall tested	Wood ratio per m^2	Infill impact	
		$K_{initiale}$	F_{max}
Kay peyi	0.18	Yes	Yes
Pombalino [16]	0.43	Yes	No
Dhajji-Dewari [12]	0.29	Yes	No
Maso [37]	0.39	Yes	Yes

The "Pombalino" wall is illustrated in Fig. 21) and was studied in Meireles et al. [16] in which three shear wall tests were performed. The structure is compounded by continuous beams and posts connected to one another by cross halving joints, as displayed in Fig. 22(c). It is braced by X-crosses and filled by hydraulic lime interspersed with tiles and broken bricks. cross-sectional area measured 16×8 cm^2; 12×8 cm^2 and 10×7 cm^2 section area. The nails were all pyramidal, 12.5 cm long with a base section of 10×6 mm^2. The nails used to connect the crossed braces to each other were smaller, measuring 7.5 cm long with a base section of 5×5 mm^2. A 7.5 mm hole was pre-drilled in the upper wooden element.

Three Dhajji-Dewari walls were constructed from three sets of members, with cross-sectional dimensions of 10×10 cm^2, 5×10 cm^2 and 2.5×10 cm^2. The plain shank nails were made of mild steel and measured 75 mm long on the top and bottom beams and 50 mm long elsewhere. The infill exhibited a different stone-to-mud ratio depending on the test specimen. This framework is depicted in Fig. 23 and was studied in Ali et al. [12].

As for the Maso wall, the posts display a cross-section of approximately 16×16 cm^2, with nailed lapped joints. The wooden joints are held by a pair of normal wood screws rather than the traditional nails with a square cross-section. The diagonal planks have

a cross-section of approximately 7×16 cm^2 and are devoid of connections, instead simply being rested against the inside of the beams. The infill is composed of crushed stone (with a very large particle size) held together using a mortar made of lime, earth and sand. The structure of this wall is displayed in Fig. 24 and was studied in Ceccotti et al. [37].

The main values and observations from these tests are presented in Tables 11 and 12. Table 11 lists the type of joint used in the framework and type of element where failure first appeared; it also summarizes the drift ratio attained for the maximum load F_{max}. F_{max} values obviously differ and it is not relevant to directly compare them to one another given the geometric and technical details that vary according to the type of wall. Nevertheless, this comparison yields information relative to the corresponding drift, in addition to providing the EVD whenever possible. Table 12 shows whether or not the infill exerts an influence on the structural behavior.

The following observations have been drawn from this comparison:

- Drift: for the four frameworks studied herein, the drift range for F_{max} is approx. 2.0–2.5% except for the value of the "kay peyi" shear wall which is 3.0% even though no vertical loading was applied on the structure. The first specimens are traditional buildings, whereas the last one has been adapted from the Haitian building cultures and therefore features some technical improvements, such as the steel strip that allows for this large value of drift.
- EVD: this coefficient has only been calculated in Ali et al. [12]; it indicates that the mean value is very close to the kay peyi wall. On the other hand, Ali et al. [12] observed that for the empty wall, this value was lower, *i.e.* equal to 7% as opposed to 16% for the Haitian configuration. This discrepancy can be explained by the fact that the Dhajji-Dewari walls contain a high ratio of wood (see Table 12) which prevents the wood structure from being highly dissipative. This also suggests that the infill possesses a significant energy dissipation capacity.
- Infill influence: Table 12 summarizes the observations and assumptions relative to the influence of infill on the initial stiffness and maximum load displayed by the wall for the four types of structures described above. According to Ali et al. [12] and Meireles et al. [16], infill exerts no or only limited impact on the lateral load capacity of the wall. Regarding the Dhajji-Dewari structure studied in the first article, this lack of impact is due to the dimensions of the elementary cell: for the first structure, the cell is 53.8 cm high and 67.5 cm wide (interior dimensions). Hence, the wood structure is denser, with 29% of wood per m^2 in comparison with the kay peyi wall studied herein (at 18%) and therefore behaves as a lattice. For the Pombalino "frontal" walls, cell is a square 1.2 m wide but the entire wood structure is made of continuous beams connected together by cross halving joints (see Fig. 22(c)) that prevent large deformations from forming in the timber frame. Furthermore, the wood cross-sections are large since the wood ratio equals 0.43, hence the wood frame also behaves like a lattice. In relation to the Maso wall, Ceccotti et al. [37] did not analyze the influence of infill given that the diagonal members are not linked to the vertical posts and are thus free to move without infill. In this case, the infill is structurally necessary.

This discussion demonstrates that while the structures seem to be similar, their geometric and technical details make their corresponding structural responses quite different.

5. Conclusion

This paper has presented a multi-scale experimental program, during which a connection, an elementary cell and a shear wall have been tested; moreover, results were compared with other experimental studies on the same type of structures.

At scale 1, both normal and tangential tests were conducted on the type-1 connection. The first specimens exhibit a resistance nearly proportional to the number of nails. It was also found that using plain shank nails in rural parts of Haiti for wood construction is indeed relevant, given the nail pull-out behavior as well as their low price relative to the local context.

At scale 2, many tests were completed in order to analyze the influence of infill, type of infill and bracing. These results show that at this scale, infill and hence the type of infill exert no impact on the lateral load capacity, but only on the initial stiffness due to the very lattice-like behavior exhibited by the elementary cell, which in turn reveals that infill offers a low lateral load capacity.

At scale 3, shear wall tests demonstrated the benefit of infill and the high ductility of these filled wood structures. Moreover, the load–drift curve highlights the significant pinching effect, which allows considering that the specimens would perform well if exposed to a seismic hazard.

The structure studied herein was then compared with other traditional construction types that make use of the same building materials. This analysis revealed that the timber framework presented in the studied structure has very high ductility in comparison to the other configurations due to the type-1 connection, which can experience significant deformation and dissipate a large amount of energy. In that way, this work tends to confirm the good seismic resistant behavior exhibited by the timbered masonry structures.

This experimental program has yielded some highly relevant results in performing multi-scale modeling for the purpose of predicting the behavior and assessing the vulnerability of Haitian structures under seismic loading.

In order to strengthen these observations and validate the multi-scale approach, another experimental program on the shear wall and at a complete Haitian house (scale 4) will be performed dynamically on a shaking table.

Acknowledgement

The authors wish to thank and acknowledge the support of the French National Research Agency (ANR) under reference code ANR-10-HAIT-003, the Haitian association GADRU, the participating associations of the PADED platform and all local partners for their involvement and participation, contributing to this research project. The authors also thank the technical staffs at both Trento/CNR Ivalsa and Grenoble/UJF for the tests they conducted. Gratitude is extended to Simon Pla and Patrice Clavel for their valuable assistance during the experimental program on the elementary cell.

References

[1] Gurpinar A, Erdik M, Ergunay O. Siting and structural aspects of adobe buildings in seismic areas. In: Earthen buildings in seismic areas. Proceedings of the international workshop held at the university of New Mexico, Albuquerque, May 24–28, 1981. National Science Foundation; 1981. p. 139–83.
[2] Langenbach R. From "Opus Craticium" to the "Chicago Frame": earthquake-resistant traditional construction. Int J Archit Heritage 2007;1(1):29–59.
[3] Caimi A. Cultures constructives vernaculaires et résilience. Entresavoir, pratique et technique: appréhender le vernaculaire en tant quegénie du lieu et génie parasinistre, Ph.D. thesis, Ecole NationaleSupérieure d'Architecture de Grenoble, 2014.

[4] Gutierrez J. Notes on the seismic adequacy of vernacular buildings. In: 13th World conference on earthquake engineering; National science foundation, 2004. p. 1–6.
[5] Copani P. Timber-frame buildings in Scandinavia: high deformation prevent the system from collapse. In: From material to structure – mechanical behaviour and failures of the timber structures, ICOMOS IWC – XVI international symposium; The ICOMOS International Wood Committee (IIWC), 2007.
[6] Dutu A, Ferreira J, Guerreiro L, Branco F, Goncalves A. Timbered masonry for earthquake resistance in Europe. Mater Constr 2012;62(308):615–28.
[7] Paultre P, Calais É, Proulx J, Prépetit C, Ambroise S. Damage to engineered structures during the 12 January 2010, Haiti (Léogâne) earthquake 1. Can J Civil Eng 2013;40(999):1–14.
[8] Tobriner S. Wooden architecture and earthquakes in Turkey: a reconnaissance report and commentary on the performance of wooden structures in the Turkish earthquakes of 17 August and 12 November 1999. In: International conference on the seismic performance of traditional buildings, The ICOMOS International Wood Committee (IIWC), Istanbul, Turkey; November 16–18, 2000.
[9] Makarios T, Demosthenous M. Seismic response of traditional buildings of Lefkas Island, Greece. Eng Struct 2006;28(2):264–78.
[10] Langenbach R. Learning from the past to protect the future: Armature Crosswalls. Eng Struct 2008;30(8):2096–100.
[11] Audefroy JF. Haiti: post-earthquake lessons learned from traditional construction. Environ Urban 2011;23(2):447–62.
[12] Ali Q, Schacher T, Ashraf M, Alam B, Naeem A, Ahmad N, Umar M. In-plane behavior of full scale Dhajji Walls (Wooden Braced with Stone Infill) under quasi static loading. Earthq Spectra 2012;28(3):835–58.
[13] Ferreira J, Teixeira M, Duţu A, Branco F, Gonçalves A. Experimental evaluation and numerical modelling of timber-framed walls. Exp Tech 2012.
[14] Cruz H, Moura JP, Machado JS. The use of FRP in the strengthening of timber reinforced masonry load-bearing walls. In: Historical constructions, Guimar aes, vol. 847. Universidade do Minho, Portugal: Paulo B. Lourenço/ Universitat Politècnica de Catalunya, Spain: Pere Roca. 2001.
[15] Vasconcelos G, Poletti E, Salavessa E, Jesus AM, Loureno PB, Pilaon P. In-plane shear behaviour of traditional timber walls. Eng Struct 2013;56(0):1028–48. ISSN 0141-0296.
[16] Meireles H, Bento R, Cattari S, Lagomarsino S. A hysteretic model for frontal walls in Pombalino buildings. Bull Earthq Eng 2012;10(5):1481–502.
[17] Poletti E, Vasconcelos G. Seismic behaviour of traditional half-timbered walls: cyclic tests and strengthening solutions. J Heritage Conserv 2012;32:137–42.
[18] Ceccotti A, Faccio P, Nart M, Simeone P. Seismic behavior of wood framed buildings in Cadore mountain regioni – Italy. In: 13th World conference on earthquake engineering; Vancouver, B.C., Canada, Paper No. 4011, 2004. 14p.
[19] Langenbach R. Preventing pancake collapses: lessons from earthquake-resistant traditional construction for modern buildings of reinforced concrete. In: International disaster reduction conference (IRDC), Davos, Switzerland; 2006.
[20] Langenbach R, Kelley S, Sparks P, Rowell K, Hammer M. Preserving Haiti's Gingerbread Houses. Earthquake Mission Report. New York, NY: World Monuments Fund; 2010.
[21] Langenbach R. Don't tear it down!: preserving the earthquake resistant vernacular architecture of Kashmir, Oinfroin Media, 2009.
[22] Schacher T. Dhajji Research Project - Report of field visit in Pakistan, institute for Applied Sustainability to the Built Environment, University of Applied Sciences of Southern Switzerland, 2008.
[23] Küçükerman O, Güner S. Turkish houses in Anatolian heritage, Book for ministry of Turkish culture.
[24] Aktas YD, Akyüz U, Türer A, Erdil B, Sahin Güçhan N, Seismic resistance evaluation of traditional Ottoman timber-frame himis houses: Frame loadings and material tests, Earthquake Spectra.
[25] Kouris LAS, Kappos AJ. Detailed and simplified non-linear models for timber-framed masonry structures. Journal of Cultural Heritage 2012;13(1):47–58.
[26] Betbeder-Matibet J. La casa baraccata. Guida al progetto e al cantiere di restauro, Roma: GBeditoria; 2010.
[27] Langenbach R. "Crosswalls" instead of shearwalls, in: 5th National Conference on Earthquake Engineering, 2003.
[28] Dogangun A, Tuluk O, Livaoglu R, Acar R. Traditional wooden buildings and their damages during earthquakes in Turkey. Eng Fail Anal 2006;13(6): 981–96.
[29] EN 338, Structural timber – strength classes; 2003.
[30] EN 10230-1, Steel wire nails – Part 1: loose nails for general applications; 2000.
[31] ISO 21581, Timber structures – static and cyclic lateral load test methods for shear walls; 2010.
[32] EN 12512, Timber structures – test methods – cyclic testing of joints made with mechanical fasteners; 2002.
[33] Fonseca FS, Rose SK, Campbell SH. Nail, Wood screw, and staple fastener connections. CUREE; 2002.
[34] Dorn M, de Borst K, Eberhardsteiner J. Experiments on dowel-type timber connections. Eng Struct 2013;47:67–80.
[35] EN 1995-1-1, Design of timber structures, Part 1-1 : general – common rules and rules for buildings; 2005.
[36] Filiatrault A, Isoda H, Folz B. Hysteretic damping of wood framed buildings. Eng Struct 2003;25(4):461–71.
[37] Ceccotti A, Faccio P, Nart M, Simeone P. Seismic behaviour of historic timber-frame buildings in the italian dolomites. In: ICOMOS international wood committee, 15th international symposium, The ICOMOS International Wood Committee (IIWC), Istanbul and Rize (Turkey), September 18–23; 2006. 16p.
[38] Humbert J, Boudaud C, Baroth J, Hameury S, Daudeville L. Multi-scalemodelling of wood shear walls. I: Calibration and validation underquasi-static reversed-cyclic loading. Engineering Structures 2014;65:52–61.